THE JOURNAL OF PHYSICAL CHEMISTRY LETTERS
A JOURNAL OF THE AMERICAN CHEMICAL SOCIETY

pubs.acs.org/JPCL

Letter

Emergence of Subsurface Oxygen on Rh(111)

Marie E. Turano, Elizabeth A. Jamka, Maxwell Z. Gillum, K. D. Gibson, Rachael G. Farber, Weronika Walkosz, S. J. Sibener, Richard A. Rosenberg, and Daniel R. Killelea*

Cite This: *J. Phys. Chem. Lett.* 2021, 12, 5844−5849

Read Online

ACCESS | Metrics & More | Article Recommendations | Supporting Information

ABSTRACT: Oxygen atoms on transition metal surfaces are highly mobile under the demanding pressures and temperatures typically employed for heterogeneously catalyzed oxidation reactions. This mobility allows for rapid surface diffusion of oxygen atoms, as well as absorption into the subsurface and reemergence to the surface, resulting in variable reactivity. Subsurface oxygen atoms play a unique role in the chemistry of oxidized metal catalysts, yet little is known about how subsurface oxygen is formed or returns to the surface. Furthermore, if oxygen diffusion between the surface and subsurface is mediated by defects, there will be localized changes in the surface chemistry due to the elevated oxygen concentration near the emergence sites. We observed that oxygen atoms emerge preferentially along the boundary between surface phases and that subsurface oxygen is depleted before the surface oxide decomposes.

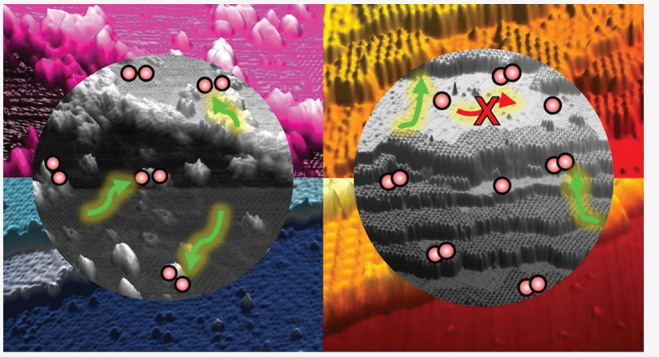

For any surface catalyzed reaction, a balance exists between the need for open sites for adsorbates and sufficient abundance of the reactant to enhance the reaction rate. Subsurface atoms absorbed into interstitial sites in the top few atomic layers of the solid offer a reservoir of reagent, without occupying the active surface sites. Their movement to the selvedge regenerates open surface sites, providing a welcoming surface to a gas-phase reactants.[1,2] Once absorbed, the presence of subsurface species may advantageously alter the electronic or geometric structure of the surface.[3] Their reemergence to the surface not only replenishes reactive adsorbates but also may cause unique reactivity due to their emergence site.[4] While catalytically active metal surfaces significantly lower the activation energy required to promote the desired reactions, elevated temperatures are still often required to drive reactions.[5,6] At higher temperatures, adsorbates are increasingly mobile. Thus, for oxidation reactions, the enhanced mobility of adsorbed oxygen atoms (O_{ad}) potentially enables them to diffuse into the subsurface via defects, creating subsurface oxygen (O_{sub}).[7−11] This rapid influx of oxygen atoms causes oxygen surface structures and compositions, as well as local electronic structures, to be highly dynamic and continuously evolving during a reaction.[9,12] Therefore, it is important to understand how the metal surface is altered by oxygen atoms emerging from the selvedge and if the process is defect-mediated or occurring stochastically across the surface.

An understanding of the emergence of O_{sub} from highly oxidized surfaces including the RhO_2 surface oxide and the surface reconstructions of the (2 × 1)-O, (2 × 2)-3O, and $(2\sqrt{3} \times 2\sqrt{3})R30°$ as well as desorption of surface oxygen from oxygen-induced surface reconstructions will provide insight into the reactivity of the metal under industrial catalytic conditions. O_{sub} are mobile O atoms dissolved in the selvedge of the metal and not strongly bound to Rh atoms as are O in the oxides.[13,14] Because O_{sub} resides in the near surface region of the metal, it can be challenging to study as its presence is often screened by surface atoms.[2,7,8,15,16] Previous studies have determined that O_{sub} participates in surface reactions,[7] enhances the rate of reaction by acting as an oxygen source,[17] and replenishes the active oxygenaceous surface phase.[10,18] Furthermore, O_{sub} formation affects the resultant surface structures by promoting the growth of oxides on the surface.[9,19,20] As defect sites and step edges on single crystal surfaces promote initial adsorption and subsequent reaction,[5,21] it follows that O_{sub} emergence could occur along step edges and defect sites, although no direct evidence of this has been observed. A recent study showed that the presence of defects alone was insufficient to form O_{sub}.[22] Rather, the primary factor in O_{sub} formation was the ability of the metal to accommodate and stabilize O_{sub}, suggesting that for a given metal there are factors beyond defects that influence the absorption and formation of O_{sub}.

Received: June 8, 2021
Accepted: June 15, 2021

https://doi.org/10.1021/acs.jpclett.1c01820
J. Phys. Chem. Lett. 2021, 12, 5844−5849

Rhodium surfaces are effective catalysts and are well-established as a model for platinum group metal reactivity. While different oxygenaceous species form on these metals, there is much commonality.[6] For example, a trilayer surface oxide forms on Rh under conditions similar to those for Ir and Pd, and the oxide trilayer has been hypothesized to form on Ru, although this has yet to be experimentally observed.[23−25] Additionally, O_2 readily dissociates on these surfaces, forming adlayers of known structure and composition.[6] While O_2 dissociates into O_{ad} on Rh(111) and saturates at an oxygen coverage (θ_O) of 0.5 monolayers (ML, 1.6×10^{15} O cm^{-2})[26] in a (2 × 1)-O adlayer, the rate of O_{sub} formation from O_{ad} is slow.[17] Furthermore, high pressures of molecular oxygen are necessary to form high oxygen phases and O_{sub}.[27,28] In order to generate higher amounts of O_{sub}, gas-phase atomic oxygen (AO) is used because it is much more likely to be absorbed. Atomic oxygen exposures at elevated temperatures result in a coexistence of the (2 × 1)-O adlayer, single-layer RhO_2 surface oxide domains, and O_{sub}. However, near room temperature, the same atomic oxygen exposures do not yield any oxide. Instead, they result in a coexistence of high oxygen content phases, namely, the (2 × 2)-3O (θ_O = 0.75 ML) and ($2\sqrt{3} \times 2\sqrt{3}$)R30° ($\theta_O$ = 0.67 ML), along with O_{sub}.[27−29]

Although the formation and stability of the various oxygenaceous species on Rh(111) are reasonably understood, it is still unclear how oxide decomposition and O_{sub} emergence are related and whether the transition between O_{sub} and O_{ad} is defect-mediated. To answer these questions, we have studied how highly oxidized Rh(111) surfaces evolve during heating using a combination of temperature-programmed desorption (TPD), scanning tunneling microscopy (STM), low-energy electron diffraction (LEED), and X-ray photoelectron spectroscopy (XPS) for oxygen quantification and surface structure characterization. We interrupted the TPD experiment at various temperatures to quench oxygen desorption and then determine the surface structures at that temperature. Strikingly, the growth of oxide on the surface did not appear to be limited to defect sites and step edges; rather, it also occurred on the terraces as a result of surface phase transitions stimulating the emergence of O_{sub}.

We first looked at how the surface changed with increasing temperature when starting with the (2 × 1)-O adlayer and no O_{sub} as shown in the Supporting Information. This understanding of how the decomposition of the (2 × 1)-O adlayer appeared in STM images and LEED allows us to compare to the behaviors of O_{ad} alone to the higher oxygen surface preparations (>0.5 ML O) with other oxygenaceous species present. Also, the saturation coverage after O_2 exposure resulting in 0.5 ML was used to calculate θ for higher O coverages by integration of the TPD spectra. We observed that, as the surface was heated, O_{ad} recombined and desorbed as O_2, causing the (2 × 1)-O adlayer to vanish. The acquired STM images (Figures S1 and S2) show a speckled surface with some scattered domains of (2 × 2)-O (θ_O = 0.25 ML), O_{ad} (dark spots), and Rh adatoms (bright patches). There is, however, no evidence of oxide formation or any difference in surface evolution near steps when compared to the middle of terraces. As anticipated, between surface temperatures (T_s) of 800 and 1000 K, θ_O decreased, with a smooth evolution from the (2 × 1)-O to the speckled surface. This suggests that either recombinative desorption was uniform across the surface, or if there were preferential desorption sites, then O_{ad} species were highly mobile before desorption. Further details are provided in the Supporting Information.

Upon exposures of Rh(111) to atomic oxygen, a more aggressive oxidant than O_2, surfaces with higher θ_O and O_{sub} were prepared. As shown in Figure 1A, the exposure of

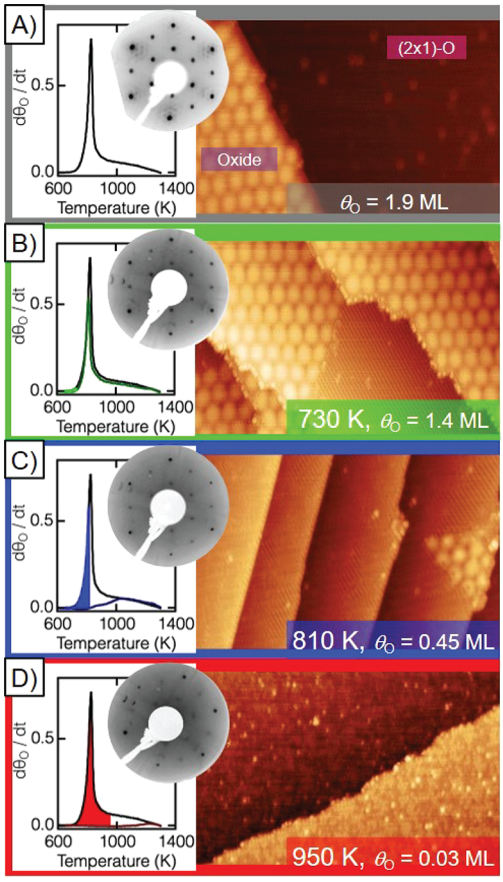

Figure 1. TPD plots, LEED patterns (62 eV), and STM images (40 × 25 nm^2) showing the evolution of Rh(111) as a function of temperature starting with (A) the initial atomic oxygen exposure, θ_O = 1.9 ML, at T_s = 700 K and then ramping the temperature to (B) 730 K, (C) 810 K, and (D) 950 K. θ_O of the STM images was determined from integration of the respective TPD. Image conditions: (A) 400 mV, 400 pA; (B) 390 mV, 370 pA; (C) 460 mV, 370 pA; and (D) 390 mV, 370 pA.

Rh(111) to atomic oxygen at T_s = 700 K yielded brims of the surface oxide (RhO_2) on the upper terrace along step edges and domains of the (2 × 1)-O adlayer elsewhere. Evidence for the surface oxide was indicated by splitting of the (1 × 1) LEED spots (shown in Figure 1A and Figure S7) and large (≈24 Å) bright hexagonal features in the STM images that were the result of a Moiré pattern of the (8 × 8) RhO_2 over (9 × 9) Rh.[25] The (2 × 1)-O adlayer appears as straight rows of alternating light and dark lines. Heating to 730 K, just before the onset of the sharp desorption peak as seen in the TPDs in Figure 1, reduced θ_O to 1.4 ML, indicating a modest amount of O desorption (Figure 1B). STM images showed that heating to 730 K caused the (2 × 1)-O domains to become more ordered, with some bright spots appearing on the step-down side of the surface oxides. The portion of the surface oxide bordering the (2 × 1)-O adlayer also showed a slight disruption. Together, these changes suggest that O_{sub} emergence occurred around the perimeter of the RhO_2 surface

https://doi.org/10.1021/acs.jpclett.1c01820
J. Phys. Chem. Lett. 2021, 12, 5844−5849

oxide and induced 1-D oxide formation along the step edge.[20] The activity along the perimeter was previously attributed to enhanced catalytic oxidation of CO, albeit at significantly lower temperatures.[30]

The STM images taken at different temperatures during the TPD experiment show that, as the oxide domains diminished, they were replaced by domains of the (2 × 1)-O adlayer. θ_O decreased to 0.45 ML at 810 K (Figure 1C) and 0.03 ML at 950 K (Figure 1D). The LEED patterns concomitantly showed the persistence of the (2 × 2) pattern, indicative of the (2 × 1)-O adlayer, and the disappearance of the oxide splitting about the (1 × 1) spots. Figure 1C showed that only small patches of the surface oxide remained along the step edges, and the (2 × 1)-O adlayer was largely unperturbed. These observations suggest that O_{sub} was depleted before significant oxide decomposition occurred, because small oxide patches were still observed after the 850 K ramp, where θ_O was less than 0.5 ML indicating that all O was either on the surface or in the oxide. However, this process did not disrupt the (2 × 1)-O adlayer. As shown in Figure 1D, a further decrease of θ_O gave the same speckled surface observed at this temperature when starting from the 0.5 ML O_{ad} surface. The area of the domain boundary between the oxide and the (2 × 1)-O adlayer was more important for O_{sub} emergence than the presence of steps as defect sites. The evolution of this mixed metallic oxide surface showed that O_{sub} emergence along the perimeter of the surface oxide was strongly favored over emergence on the terraces.

We then looked at how a surface without the oxide evolved as a result of O_{sub} emergence during heating. Exposure of Rh(111) to atomic oxygen at T_s = 350 K yielded θ_O = 1.4 ML and a surface covered in a mixture of the $(2\sqrt{3} \times 2\sqrt{3})R30°$ and (2 × 2)-3O structures with the remaining oxygen dissolved into the selvedge as O_{sub}. As shown in Figure 2A, the LEED was distorted from the (2 × 2) pattern, agreeing with previous work.[28,29] We have previously shown that annealing this surface to T_s = 700 K resulted in a largely (2 × 1)-O covered surface with some oxide growth from the steps seen in STM images.[29] The appearance of patches of oxide suggested that they grew from nucleation sites, as often occurs on other late transition metal surfaces.[23] A (2 × 2) LEED pattern was observed after annealing, indicating the transition to the (2 × 1)-O adlayer with some oxidic growth.[29] However, in those experiments, θ_O was constant (e.g., no O_2 desorption occurred). In the present case, we investigated how the surface responded to higher temperatures where θ_O decreased and O_{sub} was driven from the selvedge. The surface was ramped to elevated temperatures corresponding to the onset of oxygen desorption (T_s = 760 K, Figure 2B), near the apex of the sharp desorption peak (T_s = 830 K, Figure 2C, and 850 K, Figure 2D), and after the sharp desorption peak (T_s = 950 K, Figure 2E) as seen in the TPDs in Figure 2. The STM images show that T_s = 760 K was sufficient for the (2 × 1)-O adlayer to supplant the mixed phases and induce the formation of small patches of oxide, as evidenced by the bright patches in the STM images which correspond to oxide patches, not Rh metal islands, as further detailed in Figure S6. The LEED patterns support the STM observations as a (2 × 2) LEED pattern was also observed.

The XPS data shown in Figure 3 confirm that oxide was formed upon heating. Figure 3A shows the O 1s region after an atomic oxygen exposure at T_s = 350 K, and the peak was fit using two components, a larger component at 529.6 eV that

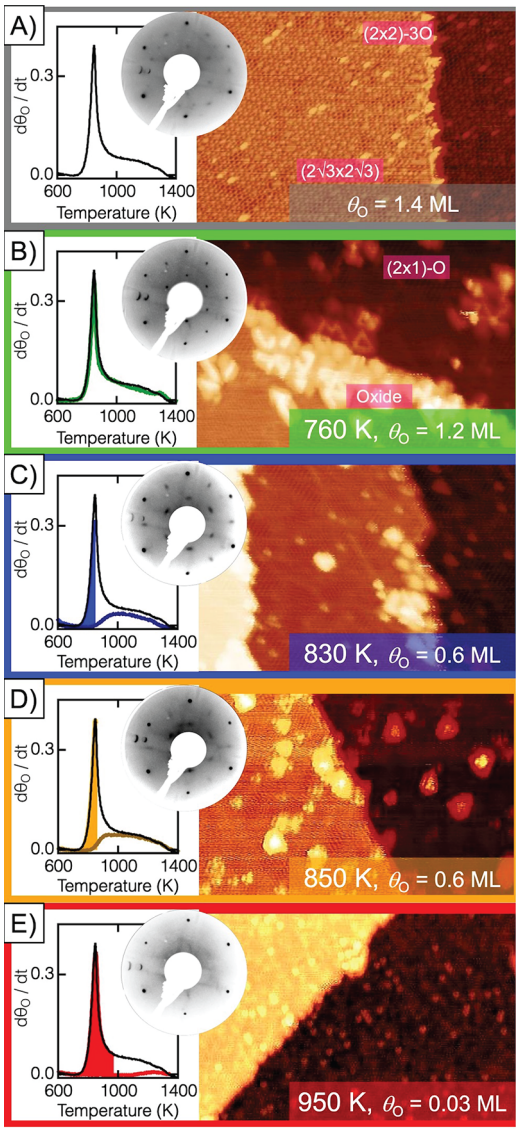

Figure 2. TPD plots, LEED patterns (62 eV), and STM images (40 × 25 nm^2) showing the evolution of Rh(111) as a function of temperature starting with (A) the initial atomic oxygen exposure, θ_O = 1.4 ML, at T_s = 350 K and then ramping the temperature to (B) 760 K, (C) 830 K, (D) 850 K, and (E) 950 K. θ_O of the STM images was determined from integration of the respective TPD. Imaging conditions were (A) 400 mV, 400 pA; (B) 440 mV, 360 pA; (C) 380 mV, 340 pA; (D) 300 mV, 260 pA; and (E) 660 mV, 440 pA.

corresponded to O_{ad} and O atoms in the lower layer of the RhO_2 oxide as well as a smaller peak at 528.8 eV that corresponded to O in the upper layer of the RhO_2 surface oxide.[27,28] Further details about the XPS experimental procedures and spectral deconvolution are provided in the Supporting Information. Figure 3B shows the XPS obtained after annealing at 700 K for 600 s in UHV. The O 1s region was fit by the same two components as in Figure 3A. It is clear that the O 1s component at 528.8 eV, which arises solely from the surface oxide, became more pronounced, agreeing well with the STM images in Figure 2B taken after stopping the TPD ramp at 760 K. Together, the STM images and XPS spectra indicate that heating caused the formation of the RhO_2 surface oxide.

https://doi.org/10.1021/acs.jpclett.1c01820
J. Phys. Chem. Lett. 2021, 12, 5844−5849

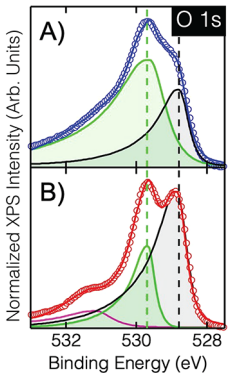

Figure 3. O 1s XPS of Rh(111) after (A) atomic oxygen exposure at T_s = 350 K; followed by (B) 600 s anneal at T_s = 700 K. The green shaded peak includes the O_{ad} component (529.6 eV, green dashed line), and the black shaded peak is exclusively the oxide component (528.8 eV, black dashed line). The solid circles are data, and the solid lines are fits to the data from adding together the individual components. The minor component (pink) around 531 eV was likely surface OH.

From STM imaging, we consistently observed oxide formation on the terraces as well as along the steps. Figure 2B shows that although θ_O decreased to 1.2 ML due to some O_2 desorption, oxidic patches appeared, while the (2 × 1)-O adlayer was present at the surface. The oxide could not have arisen from conversion of the surface phases alone as there is insufficient O in the surface phase to form both the oxide and the (2 × 1)-O adlayer. Therefore, we attribute the oxide formation to the emergence of O_{sub} onto the terraces. As O_{sub} diffused to the surface from the selvedge, the local concentration of oxygen increased, causing oxide nucleation. Because the surface temperature (T_s = 760 K) was below the peak decomposition temperature of 825 K for the RhO_2 oxide, instead of desorbing, the emergent O_{sub} became incorporated into these small oxide patches. The oxide growth along the step edge indicates that O_{sub} emergence was enhanced by these surface defects, and the oxide grew out from both the upper and lower terrace. However, the observation of oxide scattered on the terrace indicates that there must have been other pathways for O_{sub} emergence than just steps, namely, the terrace. We propose that O_{sub} emergence was spurred by surface phase transitions.

As the temperature was further increased to 950 K, the surface evolved in a similar fashion as the surface with mixed oxide and the (2 × 1)-O adlayer. By 830 K (Figure 2C), with θ_O = 0.6 ML, O_{sub} was exhausted, and a smaller amount of the oxide was evident in the STM images. From this point on, the behavior was the same for all initial preparations. At 850 K, Figure 2D, the STM images showed that the oxide patches further decreased in size and number, with no apparent difference in the behavior between the terraces and the step edges. The image in Figure 2E shows that, as θ_O decreased to 0.03 ML (950 K), the surface was disordered: the (2 × 1)-O domains were gone, and the surface was covered with scattered O_{ad} and Rh metallic islands. The presence of steps did not have any observed effect on the oxide decomposition or the surface species present. Altogether, these results show that once O_{sub} was removed, no matter the initial preparation, all surfaces behaved similarly and were virtually indistinguishable when θ_O decreased below 0.5 ML.

These observations show where O_{sub} emerges on the surface. It is believed that O_{sub} plays a key role in regulating oscillating catalytic reactions, as its formation and emergence establish the passive and active surface phases.[1,10,12,18] Oxide growth has been attributed to oxygen atoms diffusing into the selvedge at steps, providing steric access to Rh atoms on the upper terrace to form the RhO_2 trilayer.[20,27,29,31,32] The present findings show that O_{sub} emerged to the surface before the surface oxide decomposed as well as before θ_O decreased appreciably; thus, the oxide is more stable than O_{sub}. When the oxide was initially present from the T_s = 700 K atomic oxygen exposures, oxide formation was not observed on the terraces. The STM images taken after the ramp to 730 K show that the surface oxide coverage was unchanged, suggesting that any desorbing O_2 was from O_{sub}, not decomposition of the oxide. Therefore, O_{sub} emergence preceded oxide decomposition. In addition, the boundary between the (2 × 1)-O adlayer and RhO_2 provided a channel for O_{sub} emergence. This resulted in an enhanced concentration of O along the oxide perimeter. These O atoms recombinantly desorbed while causing some disruption of the (2 × 1)-O adlayer along the perimeter. Without the phase transition, O_{sub} emergence was limited to defects or oxide boundaries.

In conclusion, we found that O_{sub} emerges before the desorption of other oxygenaceous surface phases and favors emerging along the oxide−metallic boundary or on the terrace if a surface phase transition occurs. O_{sub} emergence is not facilitated by defects alone. The locally elevated O concentration during emergence causes the growth of small patches of oxide to form on terraces and along steps. Once O_{sub} is depleted, the surface oxide decomposes, and the remaining oxygen recombinantly desorbs as if O_{sub} and the oxides were never present. These results indicate the need to include O_{sub} in models of heterogeneously catalyzed oxidation reactions as O_{sub} is not only a reservoir of reactive oxygen but also causes local elevated O concentrations that will have unique chemistry.

■ ASSOCIATED CONTENT

Supporting Information

The Supporting Information is available free of charge at https://pubs.acs.org/doi/10.1021/acs.jpclett.1c01820.

Experimental description, STM images, and line scans for (2 × 1)-O adlayer decomposition; STM images and line scans of both 700 and 350 K atomic oxygen exposures along with LEED patterns for the various exposures; and Argonne experimental procedures, XPS data, and Argonne LEED patterns (PDF)

■ AUTHOR INFORMATION

Corresponding Author

Daniel R. Killelea − *Department of Chemistry & Biochemistry, Loyola University Chicago, Chicago, Illinois 60660, United States;* orcid.org/0000-0001-6965-5644; Phone: +1 773 508 3136; Email: dkillelea@luc.edu

Authors

Marie E. Turano − *Department of Chemistry & Biochemistry, Loyola University Chicago, Chicago, Illinois 60660, United States*

https://doi.org/10.1021/acs.jpclett.1c01820
J. Phys. Chem. Lett. 2021, 12, 5844−5849

Elizabeth A. Jamka − *Department of Chemistry & Biochemistry, Loyola University Chicago, Chicago, Illinois 60660, United States*
Maxwell Z. Gillum − *Department of Chemistry & Biochemistry, Loyola University Chicago, Chicago, Illinois 60660, United States*
K. D. Gibson − *Department of Chemistry and The James Franck Institute, The University of Chicago, Chicago, Illinois 60637, United States*
Rachael G. Farber − *Department of Chemistry and The James Franck Institute, The University of Chicago, Chicago, Illinois 60637, United States*
Weronika Walkosz − *Department of Physics, Lake Forest College, Lake Forest, Illinois 60045, United States*
S. J. Sibener − *Department of Chemistry and The James Franck Institute, The University of Chicago, Chicago, Illinois 60637, United States;* orcid.org/0000-0002-5298-5484
Richard A. Rosenberg − *Advanced Photon Source, Argonne National Laboratory, Argonne, Illinois 60439, United States;* orcid.org/0000-0002-3346-2741

Complete contact information is available at: https://pubs.acs.org/10.1021/acs.jpclett.1c01820

Notes

The authors declare no competing financial interest.

■ ACKNOWLEDGMENTS

We wish to acknowledge support from the National Science Foundation through award CHE-1800291. M.E.T. thanks The Arthur J. Schmitt Foundation for support during this work. K.D.G., R.G.F., and S.J.S. acknowledge support from the Air Force Office of Scientific Research, Grant FA9550-19-1-0324. Use of the Advanced Photon Source was supported by the U.S. Department of Energy, Office of Science, Office of Basic Energy Sciences, under Contract DE-AC02-06CH11357.

■ REFERENCES

(1) Suchorski, Y.; Datler, M.; Bespalov, I.; Zeininger, J.; Stoger-Pollach, M.; Bernardi, J.; Gronbeck, H.; Rupprechter, G. Surface-Structure Libraries: Multifrequential oscillations in catalytic hydrogen oxidation on rhodium. *J. Phys. Chem. C* **2019**, *123*, 4217−4227.
(2) Gibson, K. D.; Viste, M.; Sanchez, E. C.; Sibener, S. J. High density adsorbed oxygen on Rh(111) and enhanced routes to metallic oxidation using atomic oxygen. *J. Chem. Phys.* **1999**, *110*, 2757−2760.
(3) Xu, Y.; Greeley, J.; Mavrikakis, M. Effect of subsurface oxygen on the reactivity of the Ag(111) surface. *J. Am. Chem. Soc.* **2005**, *127*, 12823−12827.
(4) Ceyer, S. T. The unique chemistry of hydrogen beneath the surface: Catalytic hydrogenation of hydrocarbons. *Acc. Chem. Res.* **2001**, *34*, 737−744.
(5) Somorjai, G. A.; Li, Y. *Introduction to Surface Chemistry and Catalysis*, 2nd ed.; John Wiley and Sons, Inc.: Hoboken, NJ, 2010.
(6) Weaver, J. F. Surface chemistry of late transition metal oxides. *Chem. Rev.* **2013**, *113*, 4164−4215.
(7) Wider, J.; Greber, T.; Wetli, E.; Kreutz, T. J.; Schwaller, P.; Osterwalder, J. Direct observation of subsurface oxygen on Rh(111). *Surf. Sci.* **1998**, *417*, 301−310.
(8) Peterlinz, K. A.; Sibener, S. J. Absorption, adsorption, and desorption studies of the oxygen/Rh(111) system using O_2, NO, and NO_2. *J. Phys. Chem.* **1995**, *99*, 2817−2825.
(9) Monine, M. I.; Schaak, A.; Rubinstein, B. Y.; Imbihl, R.; Pismen, L. M. Dynamics of subsurface oxygen formation in catalytic water formation on a Rh(111) surface - experiment and simulation. *Catal. Today* **2001**, *70*, 321−330.
(10) Suchorski, Y.; Datler, M.; Bespalov, I.; Zeininger, J.; Stoger-Pollach, M.; Bernardi, J.; Gronbeck, H.; Rupprechter, G. Visualizing catalyst heterogeneity by a multifrequential oscillating reaction. *Nat. Commun.* **2018**, *9*, 600.
(11) Lambeets, S. V.; Visart de Bocarmé, T.; Perea, D. E.; Kruse, N. Directional gateway to metal oxidation: 3D chemical mapping unfolds oxygen diffusional pathways in rhodium nanoparticles. *J. Phys. Chem. Lett.* **2020**, *11*, 3144−3151.
(12) Suchorski, Y.; Rupprechter, G. Local reaction kinetics by imaging. *Surf. Sci.* **2016**, *643*, 52−58.
(13) Belton, D. N.; Fisher, G. B.; DiMaggio, C. L. Identification of molecular and subsurface oxygen on stepped Rh(711). *Surf. Sci.* **1990**, *233*, 12−26.
(14) Suchorski, Y.; Zeininger, J.; Buhr, S.; Raab, M.; Stöger-Pollach, M.; Bernardi, J.; Grönbeck, H.; Rupprechter, G. Resolving multi-frequential oscillations and nanoscale interfacet communication in single-particle catalysis. *Science* **2021**, eabf8107 DOI: 10.1126/science.abf8107.
(15) Thiel, P. A.; Yates, J. T.; Weinberg, W. H. Interaction Of oxygen with the Rh(111) surface. *Surf. Sci.* **1979**, *82*, 22−44.
(16) Brault, P.; Range, H.; Toennies, J. P. Molecular beam studies of sticking of oxygen on the Rh(111) surface. *J. Chem. Phys.* **1997**, *106*, 8876−8889.
(17) Gibson, K. D.; Killelea, D. R.; Sibener, S. J. Comparison of the surface and subsurface oxygen reactivity and dynamics with CO adsorbed on Rh(111). *J. Phys. Chem. C* **2014**, *118*, 14977−14982.
(18) Winkler, P.; Zeininger, J.; Suchorski, Y.; Stoger-Pollach, M.; Zeller, P.; Amati, M.; Gregoratti, L.; Rupprechter, G. How the anisotropy of surface oxide formation influences the transient activity of a surface reaction. *Nat. Commun.* **2021**, *12*, 69.
(19) Todorova, M.; Li, W. X.; Ganduglia-Pirovano, M. V.; Stampfl, C.; Reuter, K.; Scheffler, M. Role of subsurface oxygen in oxide formation at transition metal surfaces. *Phys. Rev. Lett.* **2002**, *89*, 096103−096103a.
(20) Klikovits, J.; Schmid, M.; Merte, L. R.; Varga, P.; Westerstrom, R.; Resta, A.; Andersen, J. N.; Gustafson, J.; Mikkelsen, A.; Lundgren, E.; Mittendorfer, F.; Kresse, G. Step-orientation-dependent oxidation: from 1D to 2D oxides. *Phys. Rev. Lett.* **2008**, *101*, 266104.
(21) van der Niet, M. J. T. C.; den Dunnen, A.; Juurlink, L. B. F.; Koper, M. T. M. A detailed TPD study of H_2O and pre-adsorbed O on the stepped Pt(553) surface. *Phys. Chem. Chem. Phys.* **2011**, *13*, 1629−1638.
(22) Farber, R. G.; Turano, M. E.; Oskorep, E. C. N.; Wands, N. T.; Juurlink, L. B. F.; Killelea, D. R. Exposure of Pt(553) and Rh(111) to atomic and molecular oxygen: do defects enhance subsurface oxygen formation? *J. Phys.: Condens. Matter* **2017**, *29*, 164002.
(23) Flege, J. I.; Grinter, D. C. In situ studies of oxide nucleation, growth, and transformation using slow electrons. *Prog. Surf. Sci.* **2018**, *93*, 21−45.
(24) Diebold, U.; Li, S. C.; Schmid, M. Oxide surface science. *Annu. Rev. Phys. Chem.* **2010**, *61*, 129−148.
(25) Lundgren, E.; Mikkelsen, A.; Andersen, J. N.; Kresse, G.; Schmid, M.; Varga, P. Surface oxides on close-packed surfaces of late transition metals. *J. Phys.: Condens. Matter* **2006**, *18*, R481−R499.
(26) Turano, M. E.; Farber, R. G.; Hildebrandt, G.; Killelea, D. R. Temperature dependence of CO oxidation on Rh(111) by adsorbed oxygen. *Surf. Sci.* **2020**, *695*, 121573.
(27) Gustafson, J.; Mikkelsen, A.; Borg, M.; Lundgren, E.; Kohler, L.; Kresse, G.; Schmid, M.; Varga, P.; Yuhara, J.; Torrelles, X.; Quiros, C.; Andersen, J. N. Self-limited growth of a thin oxide layer on Rh(111). *Phys. Rev. Lett.* **2004**, *92*, 126102 DOI: 10.1103/PhysRevLett.92.126102.
(28) Kohler, L.; Kresse, G.; Schmid, M.; Lundgren, E.; Gustafson, J.; Mikkelsen, A.; Borg, M.; Yuhara, J.; Andersen, J. N.; Marsman, M.; Varga, P. High-coverage oxygen structures on Rh(111): Adsorbate repulsion and site preference is not enough. *Phys. Rev. Lett.* **2004**, *93*, 266103.
(29) Farber, R. G.; Turano, M. E.; Oskorep, E. C. N.; Wands, N. T.; Iski, E. V.; Killelea, D. R. The quest for stability: structural

dependence of Rh(111) on oxygen coverage at elevated temperature. *J. Phys. Chem. C* **2017**, *121*, 10470−10475.
(30) Farber, R. G.; Turano, M. E.; Killelea, D. R. Identification of surface sites for low-temperature heterogeneously catalyzed CO oxidation on Rh(111). *ACS Catal.* **2018**, *8*, 11483−11490.
(31) Gustafson, J.; Westerstrom, R.; Resta, A.; Mikkelsen, A.; Andersen, J. N.; Balmes, O.; Torrelles, X.; Schmid, M.; Varga, P.; Hammer, B.; Kresse, G.; Baddeley, C. J.; Lundgren, E. Structure and catalytic reactivity of Rh oxides. *Catal. Today* **2009**, *145*, 227−235.
(32) Lundgren, E.; Gustafson, J.; Resta, A.; Weissenrieder, J.; Mikkelsen, A.; Andersen, J. N.; Kohler, L.; Kresse, G.; Klikovits, J.; Biederman, A.; Schmid, M.; Varga, P. The surface oxide as a source of oxygen on Rh(111). *J. Electron Spectrosc. Relat. Phenom.* **2005**, *144*, 367−372.

https://doi.org/10.1021/acs.jpclett.1c01820
J. Phys. Chem. Lett. 2021, 12, 5844−5849